Surface waves in closed basins under parametric and internal resonances

Ali H. Nayfeh

Citation: Physics of Fluids (1958-1988) **30**, 2976 (1987); doi: 10.1063/1.866075
View online: http://dx.doi.org/10.1063/1.866075
View Table of Contents: http://scitation.aip.org/content/aip/journal/pof1/30/10?ver=pdfcov
Published by the AIP Publishing

Surface waves in closed basins under parametric and internal resonances

Ali H. Nayfeh
Department of Engineering Science and Mechanics, Virginia Polytechnic Institute and State University, Blacksburg, Virginia 24061

(Received 10 March 1987; accepted 19 June 1987)

The method of multiple scales is used to analyze the nonlinear response of the free surface of a liquid in a cylindrical container to a harmonic vertical oscillation in the presence of a two-to-one internal (autoparametric) resonance. Four first-order ordinary-differential equations are derived for the modulation of the amplitudes and phases of the two modes involved in the internal resonance with the lower mode is excited by a principal parametric resonance. In the presence of small damping, the long-time response may be any of (a) a trivial motion, (b) a limit cycle involving both modes, (c) an amplitude- and phase-modulated sinusoid (motion on a two torus), and (d) a chaotically modulated sinusoid.

I. INTRODUCTION

We consider the nonlinear response of surface waves in closed basins subject to vertical harmonic oscillations in the presence of two-to-one internal (autoparametric) resonances. The problem has relevance to liquid sloshing in liquid fuel rockets.

Faraday[1] and Rayleigh[2] studied experimentally the pattern of standing waves that appears on the surface of a container subject to harmonic vertical oscillations. They found that the surface-oscillation frequency is typically one-half that of the excitation. Benjamin and Ursell[3] analyzed the linear oscillations of this configuration assuming an irrotational inviscid fluid. They derived an infinite set of Mathieu equations and used their stability results to explain the frequency demultiplication observed by Faraday and Rayleigh.

The linear theory predicts that the parameter space $F\Omega$, where F and Ω are the amplitude and frequency of the excitation, is divided into regions of growing and decaying solutions. The predicted growth is exponential and hence the linear model is unrealistic. Consequently, a more realistic model includes nonlinear terms, which act as limiters of the response. Moreover, the linear model may predict a parametric stability (i.e., decaying response), whereas the actual response may not decay under certain conditions. In this case, the parametric excitation produces a subcritical instability that is only predictable by including nonlinear terms.

Dodge *et al.*[4] presented a finite-amplitude analysis of liquid surface oscillations in longitudinally excited rigid cylindrical containers. Miles[5] pointed out that "their equations of motion for the modal amplitudes violate reciprocity conditions that are implicit in the underlying (Newtonian) mechanics." Henstock and Sani[6] also gave a finite-amplitude analysis of surface waves in a circular container subject to periodic vertical motion. However, Henstock and Sani[6] applied the free-surface boundary conditions at the equilibrium rather than the disturbed surface and obtained a nonlinear correction to the frequency that is of first rather than second order in amplitude. Ockendon and Ockendon[7] extended the analysis of Benjamin and Ursell[3] to small but finite amplitudes, but did not calculate the parameter that measures the effects of the nonlinearity. Miles[5] extended the analysis of Ockendon and Ockendon[7] by giving an explicit expression for this parameter and by incorporating linear damping. Miles[5] also analyzed the case of a perfectly tuned two-to-one internal resonance (i.e., $\omega_2 = 2\omega_1$) when the lower mode is excited by a principal parametric resonance (i.e., $\Omega \approx 2\omega_1$), where the ω_n are the linear natural frequencies and Ω is the excitation frequency. Miles[5] did not find Hopf bifurcations and consequently, in the presence of small but finite damping, every steady-state response will be either trivial or harmonic. In this paper, we relax the perfectly tuned assumption and consider the cases $\omega_2 = 2\omega_1 + \sigma_1$ and $\Omega = 2\omega_1 + \sigma_2$, where the ω_n are the linear natural frequencies and σ_1 and σ_2 are the detuning parameters. For sufficiently nonzero values of σ_1 and σ_2, we find Hopf bifurcations, and consequently aperiodic steady-state responses.

Using an averaging technique and the Melnikov perturbation technique,[8] Holmes[9] showed that the N-degree-of-freedom model of weakly nonlinear surface waves proposed by Miles[10] has transverse homoclinic orbits in the presence of a two-to-one internal resonance. Consequently, Smale horseshoes, and hence sets of chaotic orbits exist in the phase plane and an irregular sloshing of energy takes place between the two modes of oscillation involved in the internal resonance.

Recently, a number of experiments[11–15] have been conducted to detect irregular or chaotic motions on the surfaces of liquids in containers subject to periodic vertical oscillations. Using liquid helium and water in thin annular troughs, Keolian and co-workers[11,13] observed period doubling as well as quasiperiodic surface waves involving three modes. Gollub and Meyer[12] examined the loss of stability of a single axisymmetric mode and its period-doubling bifurcations. At relatively high amplitudes, Gollub and Meyer[12] observed temporal chaos with azimuthal spatial modulation. Ciliberto and Gollub[14,15] examined the case in which the excitation amplitude and frequency are near the intersection of the stability boundary between two degenerate modes and found that they can compete to produce either periodic or chaotic motion. Our weakly nonlinear analysis may not apply to these strongly nonlinear observations.

 0031-9171/87/102976-08$01.90

II. PROBLEM FORMULATION

We consider the nonlinear surface oscillations of a liquid that fills a rigid cylindrical container to a quiescent depth d^* when the container is excited longitudinally. The fluid is assumed to be inviscid and its motion to be irrotational so that its velocity can be derived from a potential function. The influence of surface tension on the surface motion is neglected. Distances are made dimensionless using a characteristic length l of the cross section of the container and time is made dimensionless using the characteristic time $(l/g)^{1/2}$, where g is the gravitational acceleration.

Let x, y, z be a Cartesian coordinate system fixed with the container so that x and y lie in the undisturbed free surface and z is positive away from the bottom of the container. Then, the velocity $\mathbf{v}$ can be expressed in terms of the velocity potential $\phi(x,y,z,t)$ as

$$\mathbf{v} = \nabla\phi + \frac{\partial\phi}{\partial z}\mathbf{k}, \quad \nabla\phi = \frac{\partial\phi}{\partial x}\mathbf{i} + \frac{\partial\phi}{\partial y}\mathbf{j}, \tag{1}$$

where $\mathbf{i}$, $\mathbf{j}$, and $\mathbf{k}$ are unit vectors in the x, y, and z directions, respectively. For an incompressible fluid, $\operatorname{div}\mathbf{v} = 0$, and hence ϕ satisfies Laplace's equation, namely,

$$\nabla^2\phi + \frac{\partial^2\phi}{\partial z^2} = 0. \tag{2}$$

The no-penetration condition demands that the fluid velocity normal to the container walls and bottom must be zero. Consequently,

$$\frac{\partial\phi}{\partial z} = 0 \quad \text{at } z = -d \tag{3}$$

and

$$\nabla\phi\cdot\mathbf{n} = 0 \quad \text{on } \delta S, \tag{4}$$

where $d = d^*/l$, δS is the surface of the container cross section S, and $\mathbf{n}$ is the outwardly directed normal to the container. The kinematic condition that every fluid particle on the surface remains on the surface yields

$$\frac{\partial\eta}{\partial t} - \frac{\partial\phi}{\partial z} + \nabla\phi\cdot\nabla\eta = 0 \quad \text{at } z = \eta, \tag{5}$$

where $z = \eta(x,y,t)$ is the disturbed free surface. Balance of the normal stresses at the free surface yields

$$\frac{\partial\phi}{\partial t} + (1+\ddot{z}_0)\eta + \frac{1}{2}\left[(\nabla\phi)^2 + \left(\frac{\partial\phi}{\partial z}\right)^2\right] = 0 \quad \text{at } z = \eta, \tag{6}$$

where $\ddot{z}_0$ is the dimensionless acceleration of the container.

The solution of Eq. (2) that satisfies Eqs. (3) and (4) is

$$\phi(x,y,z,t) = \sum \phi_m(t)\psi_m(x,y)\operatorname{sech} k_m d \cosh k_m(z+d). \tag{7}$$

Here, the ψ_m are the linear normal mode shapes; they are governed by

$$\nabla^2\psi_m + k_m^2\psi_m = 0, \tag{8}$$

subject to the condition

$$\nabla\psi_m\cdot\mathbf{n} = 0 \quad \text{on } \delta S. \tag{9}$$

The ψ_m are orthonormalized so that

$$\iint \psi_m\psi_n\,dS = \delta_{mn}S, \tag{10}$$

where δ_{mn} is the Kronecker delta. In Eq. (7) and what follows, the summation sign indicates summation over the repeated dummy indices. We expand the free-surface elevation in terms of the ψ_m as

$$\eta(x,y,t) = \sum \eta_m(t)\psi_m(x,y). \tag{11}$$

To impose the boundary conditions Eqs. (5) and (6), we first transfer these boundary conditions from $z = \eta$ to $z = 0$ using Taylor-series expansions. Thus we replace them with

$$\frac{\partial\eta}{\partial t} - \frac{\partial\phi}{\partial z} - \frac{\partial^2\phi}{\partial z^2}\eta + \nabla\phi\cdot\nabla\eta + \cdots = 0 \quad \text{at } z = 0, \tag{12}$$

$$\frac{\partial\phi}{\partial t} + \frac{\partial^2\phi}{\partial t\,\partial z}\eta + (1+\ddot{z}_0)\eta + \frac{1}{2}(\nabla\phi)^2 + \frac{1}{2}\left(\frac{\partial\phi}{\partial z}\right)^2 + \cdots = 0 \quad \text{at } z = 0. \tag{13}$$

Substituting Eqs. (7) and (11) into Eqs. (12) and (13), multiplying the resulting equations by $\psi_n(x,y)$, and using the orthonormality condition Eq. (10), we obtain

$$\dot{\eta}_n - \kappa_n\phi_n + \sum(D_{nms} - k_s^2 C_{nms})\eta_m\phi_s = 0, \tag{14}$$

$$\dot{\phi}_n + \eta_n + \ddot{z}_0\eta_n + \sum\kappa_s C_{nms}\eta_m\dot{\phi}_s + \frac{1}{2}\sum(D_{nms} + \kappa_m\kappa_s C_{nms})\phi_m\phi_s = 0, \tag{15}$$

where the overdot indicates the derivative with respect to t,

$$\kappa_s = k_s \tanh k_s, \tag{16}$$

$$C_{nms} = S^{-1}\iint \psi_n\psi_m\psi_s\,dS, \tag{17}$$

$$D_{nms} = S^{-1}\iint \psi_n\nabla\psi_m\cdot\nabla\psi_s\,dS. \tag{18}$$

Integrating Eq. (18) by parts and using Green's theorem yields[10]

$$D_{nms} = \tfrac{1}{2}C_{nms}(k_m^2 + k_s^2 - k_n^2). \tag{19}$$

Eliminating the ϕ_n from Eqs. (14) and (15) and invoking Eq. (19) yields

$$\ddot{\eta}_n + \omega_n^2\eta_n + \kappa_n\ddot{z}_0\eta_n + \sum\Gamma_{nms}\eta_m\ddot{\eta}_s + \sum\chi_{nms}\dot{\eta}_m\dot{\eta}_s = 0, \tag{20}$$

where

$$\omega_n^2 = \kappa_n, \tag{21}$$

$$\Gamma_{nms} = \tfrac{1}{2}\kappa_n C_{nms}[2 + (k_m^2 - k_n^2 - k_s^2)/\kappa_n\kappa_s], \tag{22}$$

and

$$\chi_{nms} = \frac{1}{2}\kappa_n C_{nms}\left(1 + \frac{k_m^2 + k_s^2 - k_n^2}{2\kappa_m\kappa_s} + \frac{k_m^2 - k_n^2 - k_s^2}{\kappa_n\kappa_s}\right). \tag{23}$$

Equations (20) are in full agreement with those derived by Miles[10] using a Lagrangian formulation. In fact, Eqs. (20)

can be derived from the Lagrangian

$$L=\frac{1}{2}\kappa_n^{-1}(\dot{\eta}_n^2-\omega_n^2\eta_n^2)-\frac{1}{2}\ddot{z}_0\eta_n^2+\frac{1}{2}\sum a_{nms}\eta_n\dot{\eta}_m\dot{\eta}_s \tag{24}$$

of Miles,[10] where

$$a_{nms}=C_{nms}[1+(k_n^2-k_m^2-k_s^2)/2\kappa_m\kappa_s]. \tag{25}$$

In this paper, we use the method of multiple scales[16,17] to determine an approximate solution to Eqs. (20) for small but finite amplitudes when

$$z_0=F\cos\Omega t, \tag{26}$$

and the second natural frequency ω_2 is approximately twice the first natural frequency ω_1 and when $\Omega\approx 2\omega_1$.

III. METHOD OF SOLUTION

In this paper, we use the method of multiple scales[16,17] to determine a second-order uniform expansion of the solution of Eqs. (20) for small but finite amplitudes in the presence of a two-to-one internal resonance (i.e., $\omega_2\approx 2\omega_1$) and a principal parametric resonance of the first mode (i.e., $\Omega\approx 2\omega_1$). To express the nearness of the resonances, we introduce the detuning parameters σ_1 and σ_2 defined according to

$$\omega_2=2\omega_1+\epsilon\sigma_1 \tag{27}$$

and

$$\Omega=2\omega_1+\epsilon\sigma_2, \tag{28}$$

where ϵ is a small dimensionless parameter that is the order of the amplitude of oscillations; it serves as a bookkeeping device. Using the method of multiple scales, we seek a second-order expansion of Eqs. (20) in the form

$$\eta_n=\epsilon\eta_{n^1}(T_0,T_1)+\epsilon^2\eta_{n^2}(T_0,T_1)+\cdots, \tag{29}$$

where $T_0=t$ and $T_1=\epsilon t$. In terms of the T_n, the time derivatives become

$$\frac{d}{dt}=D_0+\epsilon D_1+\cdots$$

and (30)

$$\frac{d^2}{dt^2}=D_0^2+2\epsilon D_0D_1+\cdots,$$

where $D_n=\partial/\partial T_n$. The parametric excitation is ordered so that the effect of the parametric resonance balances the effect of the internal resonance. Thus we put

$$\Omega\kappa_n z_0=2\epsilon f_n\cos\Omega t. \tag{31}$$

We follow Miles[5] and consider the effect of weak linear damping. To this end, we add the terms $2\epsilon\mu_n\dot{\eta}_n$ in Eqs. (20). Substituting Eqs. (29)–(31) into Eqs. (20) and equating coefficients of like powers of ϵ, we obtain
order ϵ:

$$D_0^2\eta_{n^1}+\omega_n^2\eta_{n^1}=0, \tag{32}$$

order ϵ^2:

$$D_0^2\eta_{n^2}+\omega_n^2\eta_{n^2}=-2D_0D_1\eta_{n^1}-2\mu_nD_0\eta_{n^1}+2\Omega f_n\eta_{n^1}\cos\Omega T_0-\sum\Gamma_{nms}\eta_{m^1}D_0^2\eta_{s^1}-\sum\chi_{nms}(D_0\eta_{m^1})(D_0\eta_{s^1})=0. \tag{33}$$

In the presence of the weak damping, the free oscillation component of any mode that is not directly excited by the parametric resonance or indirectly excited by the internal resonance will decay with time.[18] Hence, the solution of the first-order problem (32) can be expressed in the form

$$\eta_{n^1}=A_n(T_1)e^{i\omega_nT_0}+\bar{A}_n(T_1)e^{-i\omega_nT_0} \tag{34}$$

for $n=1$ and 2 and

$$\eta_{n^1}=0,\quad \text{for } n\geqslant 3, \tag{35}$$

where $\bar{A}_n$ is the complex conjugate of A_n. Alternatively, η_{n^1} can be expressed in the form

$$\eta_{n^1}=a_n(T_1)\cos[\omega_nT_0+\beta_n(T_1)]. \tag{36}$$

Comparing Eqs. (34) and (36), we conclude that

$$A_n=\tfrac{1}{2}a_ne^{i\beta_n}, \tag{37}$$

where the a_n and β_n are the amplitudes and phases of the two modes. The functions A_n are arbitrary to this order of approximation; they are determined by imposing the solvability conditions at the next level of approximation.

Substituting Eqs. (34) and (35) into Eq. (33) yields

$$D_0^2\eta_{12}+\omega_1^2\eta_{12}=-2i\omega_1(A_1'+\mu_1A_1)e^{i\omega_1T_0}+\Omega f_1\bar{A}_1e^{i(\Omega-\omega_1)T_0}+4\omega_1\Lambda_1A_2\bar{A}_1e^{i(\omega_2-\omega_1)T_0}+\text{c.c.}+\text{NST}, \tag{38}$$

$$D_0^2\eta_{22}+\omega_2^2\eta_{22}=-2i\omega_2(A_2'+\mu_2A_2)e^{i\omega_2T_0}+\Omega f_2\bar{A}_2e^{i(\Omega-\omega_2)T_0}+4\omega_2\Lambda_2A_1^2e^{2i\omega_1T_0}+\text{c.c.}+\text{NST}, \tag{39}$$

where c.c. is the complex conjugate of the preceding terms, NST stands for terms that produce neither secular nor small-divisor terms, and

$$4\omega_1\Lambda_1=\Gamma_{121}\omega_1^2+\Gamma_{112}\omega_2^2-\omega_1\omega_2(\chi_{112}+\chi_{121}), \tag{40}$$

$$4\omega_2\Lambda_2=\omega_1^2(\Gamma_{211}+\chi_{211}). \tag{41}$$

Depending on the A_n, particular solutions of (38) and (39) may contain secular and small-divisor terms, making the expansion (29) nonuniform for large times. To obtain a uniformly valid expansion, we choose the A_n to annihilate the secular and small-divisor terms. In Sec. IV, we consider the cases $\omega_2\approx 2\omega_1$ and $\Omega\approx 2\omega_2$, and in Sec. V, we apply the results to the case of a circular cylindrical basin.

IV. PRINCIPAL PARAMETRIC RESONANCE OF THE FIRST MODE

Using Eqs. (27) and (28), we write

$$\omega_2T_0=2\omega_1T_0+\sigma_1T_1$$

and (42)

$$\Omega T_0=2\omega_1T_0+\sigma_2T_1.$$

Substituting Eq. (42) into Eqs. (38) and (39) and eliminat-

ing the terms that produce secular terms from η_{12} and η_{22} yields the solvability conditions

$$2i(A_1' + \mu_1 A_1) - 4\Lambda_1 A_2 \bar{A}_1 e^{i\sigma_1} - 2f\bar{A}_1 e^{i\sigma_2 T_1} = 0, \quad (43)$$

$$2i(A_2' + \mu_2 A_2) - 4\Lambda_2 A_1^2 e^{i\sigma_1 T_1} = 0, \quad (44)$$

where $f = f_1$. Substituting the polar form (37) into Eqs. (43) and (44) and separating real and imaginary parts, we obtain

$$a_1' + \mu_1 a_1 - \Lambda_1 a_1 a_2 \sin\gamma_1 - f a_1 \sin\gamma_2 = 0, \quad (45)$$

$$a_2' + \mu_2 a_2 + \Lambda_2 a_1^2 \sin\gamma_1 = 0, \quad (46)$$

$$-a_1\beta_1' - \Lambda_1 a_1 a_2 \cos\gamma_1 - f a_1 \cos\gamma_2 = 0, \quad (47)$$

$$-a_2\beta_2' - \Lambda_2 a_1^2 \cos\gamma_1 = 0, \quad (48)$$

where

$$\gamma_1 = \beta_2 - 2\beta_1 + \sigma_1 T_1$$

and (49)

$$\gamma_2 = \sigma_2 T_1 - 2\beta_1.$$

The steady-state solutions of Eqs. (20) correspond to the fixed points of Eqs. (45)–(49), which in turn correspond to $a_n' = 0$ and $\gamma_n' = 0$. It follows from Eq. (49) that

$$\beta_1' = \tfrac{1}{2}\sigma_2 = \nu_1$$

and (50)

$$\beta_2' = \sigma_2 - \sigma_1 = \nu_2.$$

Hence, the fixed points of Eqs. (45)–(49) are given by

$$\mu_1 a_1 - \Lambda_1 a_1 a_2 \sin\gamma_1 - f a_1 \sin\gamma_2 = 0, \quad (51)$$

$$\mu_2 a_2 + \Lambda_2 a_1^2 \sin\gamma_1 = 0, \quad (52)$$

$$-\nu_1 a_1 - \Lambda_1 a_1 a_2 \cos\gamma_1 - f a_1 \cos\gamma_2 = 0, \quad (53)$$

$$-\nu_2 a_2 - \Lambda_2 a_1^2 \cos\gamma_1 = 0. \quad (54)$$

There are two possibilities. Either

$$a_1 = a_2 = 0 \quad (55)$$

or

$$a_1^2 = \chi_1 \pm (\{f^2[\mu_2^2 + (\sigma_2 - \sigma_1)^2]/\Lambda_1^2\Lambda_2^2\} - \chi_2^2)^{1/2}, \quad (56)$$

$$a_2 = |\Lambda_2| a_1^2 [\mu_2^2 + (\sigma_2 - \sigma_1)^2]^{-1/2}, \quad (57)$$

where

$$\chi_1 = [\tfrac{1}{2}\sigma_2(\sigma_2 - \sigma_1) - \mu_1\mu_2]/\Lambda_1\Lambda_2, \quad (58)$$

$$\chi_2 = [\tfrac{1}{2}\sigma_2\mu_2 + \mu_1(\sigma_2 - \sigma_1)]/\Lambda_1\Lambda_2. \quad (59)$$

When $\chi_1 < 0$, Eq. (56) has one real root for all $f \geqslant \zeta_2$, where

$$\zeta_2 = (\mu_1^2 + \nu_1^2)^{1/2}. \quad (60)$$

In this case, there are two possible steady-state solutions: the trivial solution and a finite-amplitude solution. When $\chi_1 \geqslant 0$, Eq. (56) has one real root for all $f > \zeta_2$ and has two real roots for all $\zeta_1 \leqslant f \leqslant \zeta_2$, where

$$\zeta_1 = \Lambda_1\Lambda_2|\chi_2|[\mu_2^2 + (\sigma_2 - \sigma_1)^2]^{-1/2}. \quad (61)$$

In this case, there are three possible steady-state solutions: the trivial solution and two finite-amplitude solutions.

To determine the stability of the fixed points and hence the stability of the steady-state solutions, we let

$$A_1 = \tfrac{1}{2}(p_1 - iq_1)e^{i\nu_1 T_1}$$

and (62)

$$A_2 = \tfrac{1}{2}(p_2 - iq_2)e^{i\nu_2 T_1}$$

in Eqs. (43) and (44), separate the real and imaginary parts and obtain

$$p_1' + \mu_1 p_1 + \nu_1 q_1 - \Lambda_1(p_2 q_1 - p_1 q_2) - f q_1 = 0, \quad (63)$$

$$q_1' + \mu_1 q_1 - \nu_1 p_1 - \Lambda_1(p_1 p_2 + q_1 q_2) - f p_1 = 0, \quad (64)$$

$$p_2' + \mu_2 p_2 + \nu_2 q_2 + 2\Lambda_2 p_1 q_1 = 0, \quad (65)$$

$$q_2' + \mu_2 q_2 - \nu_2 p_2 - \Lambda_2(p_1^2 - q_1^2) = 0. \quad (66)$$

Letting $p = (p_1, q_1, p_2, q_2)^T$, we rewrite Eqs. (63)–(66) as

$$p' = F(p), \quad (67)$$

where F is a real 4-D vector function of the 4-D vector p. If $p = p_0$ is a fixed point of Eq. (67), we examine its stability by superimposing on it a disturbance $\xi(t)$ and obtain the perturbed equation

$$\xi' = F(p_0 + \xi). \quad (68)$$

Expanding Eq. (68) for small ξ, using the fact that $F(p_0) = 0$, and linearizing the resulting equation, we obtain the linear variational equation

$$\xi' = [\nabla F(p_0)]\xi. \quad (69)$$

For a fixed point to be asymptotically stable, the real parts of all of the eigenvalues of $\nabla F(p_0)$ must be negative. It follows from Eqs. (63)–(68) that the eigenvalues λ are given by

$$\begin{vmatrix} \lambda + \mu_1 + \Lambda_1 q_2 & \nu_1 - \Lambda_1 p_2 - f & -\Lambda_1 q_1 & \Lambda_1 p_1 \\ -\nu_1 - \Lambda_1 p_2 & \lambda + \mu_1 - \Lambda_1 q_2 & -\Lambda_1 p_1 & -\Lambda_1 q_1 \\ 2\Lambda_2 q_1 & 2\Lambda_2 p_1 & \lambda + \mu_2 & \nu_2 \\ -2\Lambda_2 p_1 & 2\Lambda_2 q_1 & -\nu_2 & \lambda + \mu_2 \end{vmatrix} = 0, \quad (70)$$

or

$$\begin{aligned} &\lambda_1^2\lambda_2^2 + \nu_2^2\lambda_1^2 + \lambda_2^2[\nu_1^2 - (\Lambda_1 p_2 + f)^2 - \Lambda_1^2 q_2^2] \\ &\quad + 4\lambda_1\lambda_2\Lambda_1\Lambda_2 a_1^2 + \nu_1^2\nu_2^2 \\ &\quad - \nu_2^2[(\Lambda_1 p_2 + f)^2 + \Lambda_1^2 q_2^2] \\ &\quad - 4\nu_1\nu_2\Lambda_1\Lambda_2 a_1^2 + 4\Lambda_1^2\Lambda_2^2 a_1^4 = 0, \end{aligned} \quad (71)$$

where $\lambda_n = \lambda + \mu_n$, $a_n^2 = p_n^2 + q_n^2$, and the subscript 0 was dropped for convenience of notation.

To investigate the stability of the trivial solution, we put $p_n = q_n = 0$ in Eq. (71) and obtain

$$[(\lambda + \mu_2)^2 + \nu_2^2][(\lambda + \mu_1)^2 + \nu_1^2 - f^2] = 0,$$

whose solutions are

$$\lambda = -\mu_2 \pm i\nu_2, \quad -\mu_1 \pm (f^2 - \nu_1^2)^{1/2}. \quad (72)$$

Hence, the trivial solution is stable if and only if

$$f \leqslant \zeta_2 = (\mu_1^2 + \nu_1^2)^{1/2}, \quad (73)$$

which is condition (60) for the existence of one real root of Eq. (56). It follows from Eqs. (72) and (73) that the trivial solution is a sink when $f < \zeta_2$ and a saddle when $f > \zeta_2$.

To investigate the stability of the nontrivial fixed points, we combine the steady-state equations (63) and (64) into

$$(\Lambda_1 p_2 + f)^2 + \Lambda_1^2 q_2^2 = \mu_1^2 + \nu_1^2. \quad (74)$$

Using Eq. (74), we rewrite Eq. (71) as

$$\lambda^4 + 2(\mu_1+\mu_2)\lambda^3 + (4\mu_1\mu_2+\mu_2^2+\nu_2^2+4\Lambda_1\Lambda_2 a_1^2)\lambda^2 + [2\mu_1(\mu_2^2+\nu_2^2)+4(\mu_1+\mu_2)\Lambda_1\Lambda_2 a_1^2]\lambda + 4\Lambda_1\Lambda_2 a_1^2(\Lambda_1\Lambda_2 a_1^2+\mu_1\mu_2-\nu_1\nu_2)=0. \quad (75)$$

Hence, to examine the stability of a nontrivial fixed point, we need to solve Eq. (75) and examine the real parts of its roots. Alternatively, to determine the signs of the real parts without explicitly finding the roots, we can use the Routh–Hurwitz criterion. The necessary and sufficient conditions that none of the roots of Eq. (75) have positive real parts and hence the specific fixed point is stable are

$$r_1 r_2 - r_3 > 0, \quad r_3(r_1 r_2 - r_3) - r_1^2 r_4 > 0, \quad r_4 > 0, \quad (76)$$

where r_1, r_2, r_3, and r_4 are, respectively, the coefficients of λ^3, λ^2, λ, and λ^0 in Eq. (75). The violation of the second condition implies the existence of a pair of c.c. roots with a positive real part.

V. APPLICATION OF A CIRCULAR CYLINDER

In this section, we apply the analysis of Sec. IV to the case of a circular cylinder of radius R and choose $l = R$. It follows from Eqs. (16) and (21) that the internal resonant condition $\omega_2 = 2\omega_1$ for two gravity-wave modes with dimensionless wavenumber k_2 and k_1 in a cylindrical basin with a dimensionless depth d requires that

$$k_2 \tanh k_2 d = 4k_1 \tanh k_1 d. \quad (77)$$

For a circular cylinder, condition (77) can be satisfied for several pairs of modes. The lowest such resonance for axisymmetric motion corresponds to the modes with one and three nodal circles and is given by[19]

$$k_1 = 3.8317, \quad k_2 = 10.1735, \quad d = 0.1981. \quad (78)$$

Miles[5,20] found that the coupling coefficient for this pair is rather small and he gave an example with a much larger coupling coefficient. It consists of the dominant antisymmetric and axisymmetric modes for which

$$k_1 = 1.8412, \quad k_2 = 3.8317, \quad d = 0.1523. \quad (79)$$

Thus

$$\psi_1 = N_1^{-1} J_1(k_1 r)(\sin\theta, \cos\theta), \quad (80)$$

$$\psi_2 = N_2^{-1} J_0(k_2 r), \quad (81)$$

where

$$N_1^2 = \tfrac{1}{2}(1 - k_1^{-2}) J_1^2(k_1), \quad N_2 = J_0(k_2). \quad (82)$$

Consequently,

$$C_{112} = (\pi N_1^2 N_2)^{-1} \times \int_0^1 \int_0^{2\pi} r J_1^2(k_1 r) J_0(k_2 r) \cos^2\theta \, dr \, d\theta = 0.409\,94. \quad (83)$$

The variations of ω_1, ω_2, $\epsilon\sigma_1$, Λ_1, and Λ_2 with d are shown in Table I.

It follows from Eqs. (29), (36), (42), and (49) that the fixed points correspond to the periodic solutions

$$\eta_1 = a_1 \cos(\tfrac{1}{2}\Omega t - \tfrac{1}{2}\gamma_2) + \cdots, \quad (84)$$

$$\eta_2 = a_2 \cos(\Omega t + \gamma_1 - \gamma_2) + \cdots. \quad (85)$$

TABLE I. Variation of the parameters of the modulation equations with liquid depth.

d	Λ_1	Λ_2	ω_1	ω_2	$\sigma = \omega_2 - 2\omega_1$
0.1200	−1.4133	−6.1801	0.6327	1.2835	0.0181
0.1220	−1.4612	−6.3729	0.6378	1.2927	0.0172
0.1240	−1.5099	−6.5683	0.6428	1.3019	0.0163
0.1260	−1.5592	−6.7662	0.6478	1.3109	0.0153
0.1280	−1.6094	−6.9666	0.6527	1.3198	0.0143
0.1300	−1.6602	−7.1695	0.6576	1.3285	0.0133
0.1320	−1.7117	−7.3746	0.6625	1.3372	0.0122
0.1340	−1.7639	−7.5821	0.6673	1.3457	0.0112
0.1360	−1.8167	−7.7917	0.6720	1.3541	0.0101
0.1380	−1.8702	−8.0035	0.6768	1.3624	0.0089
0.1400	−1.9244	−8.2174	0.6814	1.3706	0.0077
0.1420	−1.9791	−8.4333	0.6861	1.3787	0.0066
0.1440	−2.0345	−8.6512	0.6907	1.3867	0.0053
0.1460	−2.0905	−8.8709	0.6952	1.3946	0.0041
0.1480	−2.1470	−9.0924	0.6998	1.4023	0.0028
0.1500	−2.2041	−9.3157	0.7042	1.4100	0.0015
0.1520	−2.2618	−9.5407	0.7087	1.4175	0.0002
0.1540	−2.3200	−9.7672	0.7131	1.4250	−0.0012
0.1560	−2.3787	−9.9953	0.7175	1.4324	−0.0026
0.1580	−2.4379	−10.2248	0.7218	1.4396	−0.0040
0.1600	−2.4976	−10.4558	0.7261	1.4468	−0.0054
0.1620	−2.5578	−10.6880	0.7304	1.4539	−0.0069
0.1640	−2.6184	−10.9215	0.7346	1.4608	−0.0084
0.1660	−2.6795	−11.1562	0.7388	1.4677	−0.0099
0.1680	−2.7410	−11.3920	0.7430	1.4745	−0.0114
0.1700	−2.8029	−11.6289	0.7471	1.4812	−0.0130
0.1720	−2.8653	−11.8667	0.7512	1.4879	−0.0146
0.1740	−2.9280	−12.1054	0.7553	1.4944	−0.0162
0.1760	−2.9910	−12.3450	0.7593	1.5008	−0.0179
0.1780	−3.0544	−12.5853	0.7634	1.5072	−0.0195

The steady-state amplitudes a_n and phases γ_n depend on the five parameters f (amplitude of excitation), σ_1 (detuning of the internal resonance), σ_2 (detuning of the excitation), and the μ_n (damping coefficients). In what follows, we examine the variations of the a_n with either σ_2 or f for fixed values of σ_1, μ_1, and μ_2.

Figure 1 shows the variation of $\hat{a}_1 = a_1\sqrt{\Lambda_1\Lambda_2}/f$ and $\hat{a}_2 = a_2\Lambda_1/f$ with $\hat{\sigma}_2 = \sigma_2/f$ for $\sigma_1 = 0$ and $\hat{\mu}_n = \mu_n/f = 0.02$. In this case, the internal resonance is perfect (i.e., $\omega_2 = 2\omega_1$), corresponding to $d = 0.1523$, the case studied by

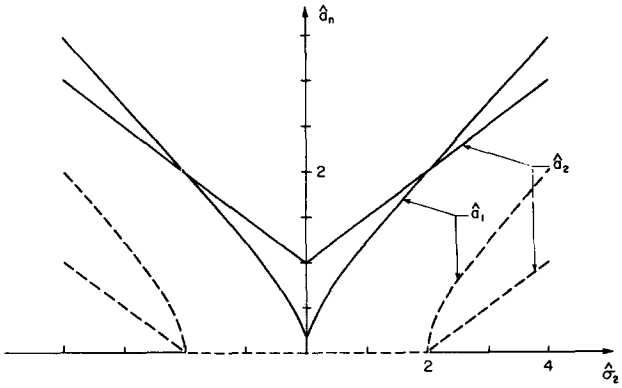

FIG. 1. Frequency-response curves for the case of principal parametric resonance of the first mode for $\sigma_1 = 0.0$ and $\mu_n/f = 0.02$: Solid curves—stable; ---, unstable with at least one eigenvalue being positive.

Miles.[5] The system response depends on the control parameter σ_2. When $-2.0<\sigma_2<2.0$, there are two possible steady-state solutions: the trivial one, which is unstable (saddle point) and a nontrivial solution, which is stable (sink). Consequently, the response is periodic. When $\sigma_2>2.0$ or $\sigma_2<-2.0$, there are three possible steady-state solutions: the trivial one, which is stable (sink) and two nontrivial solutions, the larger of which is stable (sink) and the smaller one, which is unstable (saddle point). Consequently, the response is either trivial or periodic, as given by Eqs. (84) and (85), depending on the initial conditions. Since if $\hat{a}_n$ is a solution, then $-\hat{a}_n$ is also a solution; the points $\sigma_2=2.0$ and 2.0 are subcritical pitchfork bifurcation points. As σ_2 increases past -2.0, the sink at the origin becomes a saddle point and the two saddles (corresponding to $\hat{a}_n$ and $-\hat{a}_n$) shrink toward the sink at the origin at $\sigma_2=-2.0$. Similarly, as σ_2 decreases past 2.0, the sink at the origin becomes a saddle point and the two saddles shrink toward the sink at the origin at $\sigma_2=2.0$. In this case, Hopf bifurcations do not exist, in agreement with the conclusion of Miles.[5,21]

Figure 2 shows the variation of $\hat{a}_1$ and $\hat{a}_2$ with $\hat{\sigma}_2$ for the case $\hat{\sigma}_1=0.266$, $\hat{\mu}_n=0.02$, where $\hat{\mu}_n=\mu_n/f$ and $\hat{\sigma}_n=\sigma_n/f$. When $f=0.05$, $\sigma_1=0.0133$, which corresponds to the case $d=0.13$ according to Table I. Comparing Figs. 1 and 2 shows that the detuning $\hat{\sigma}_1$ due to the internal resonance breaks down the symmetry of the frequency-response curves. An enlargement of the interval around $\hat{\sigma}_2=0.2$ is shown in Fig. 3. Inside the interval $\sigma^{(1)}\leqslant\sigma_2\leqslant\sigma^{(2)}$, where $\sigma^{(1)}\approx0.140$ and $\sigma^{(2)}\approx0.261$, the real part of a pair of c.c. eigenvalues corresponding to the nontrivial fixed points is positive. As σ_2 either increases past $\sigma^{(1)}$ or decreases past $\sigma^{(2)}$, the fixed points lose their stability, with a pair of c.c. eigenvalues crossing the imaginary axis into the right half of the complex plane. Hence, $\sigma^{(1)}$ and $\sigma^{(2)}$ are Hopf bifurcation points. Based on the Hopf bifurcation theorem,[22] near $\sigma^{(1)}$ and $\sigma^{(2)}$ the evolution equations have limit cycles with amplitudes proportional to $|\sigma_2-\sigma^{(1)}|^{1/2}$ and $|\sigma_2-\sigma^{(2)}|^{1/2}$, respectively, corresponding to 2-D tori for the original system.

Figure 4 shows the variation of $\tilde{a}_1=a_1\sqrt{\Lambda_1\Lambda_2}$ and $\tilde{a}_2=a_2\Lambda_1$ with f for a case in which Hopf bifurcations do not exist. In this case, $\mu_1=\mu_2=0.002$, $\sigma_1=0.0133$ (corresponding to $d=0.13$), and $\sigma_2=0.04$. When $f<\zeta_1$, the trivial solution is the only possible fixed point, which is stable (sink). When $f>\zeta_2$, there are two possible fixed points: a trivial point, which is unstable (saddle point) and a nontrivial point, which is stable (sink). Consequently, the response is periodic and given by Eqs. (84) and (85). When $\zeta_1<f<\zeta_2$, there are three possible fixed points: a trivial point, which is stable (sink) and two nontrivial points, the larger of which is stable (sink) and the smaller one, which is unstable (saddle point). Consequently, the response is either periodic or trivial depending on the initial conditions. When $f<\zeta_1$, only the trivial solution is possible, which is stable (sink). Consequently, the response is trivial. The point $f=\zeta_1$ is a saddle-node bifurcation point. Two branches of steady states emerge from the bifurcation point: one stable (node) and one unstable (saddle point). For the basic system, $f=\zeta_1$ is a cyclic fold. When $\zeta_1<f<\zeta_2$, two periodic solutions (limit cycles) of different stability coexist. As f decreases, the two limit cycles approach one another and collide at $f=\zeta_1$. As f decreases below ζ_1, both solutions disappear and the response is trivial. The point $f=\zeta_2$ is a subcritical pitchfork bifurcation point. As f increases toward ζ_2,

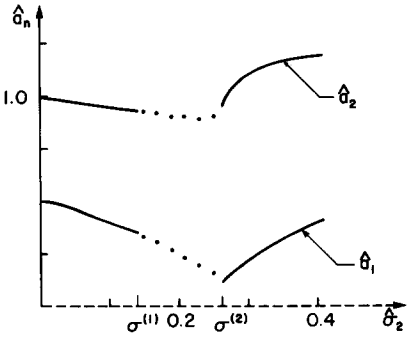

FIG. 3. Frequency-response curves for the case of principal parametric resonance of the first mode for $\sigma_1/f=0.266$ and $\mu_n/f=0.02$: Solid curves — stable; ---, unstable with at least one eigenvalue being positive; ···, unstable with the real part of a c.c. pair of eigenvalues being positive.

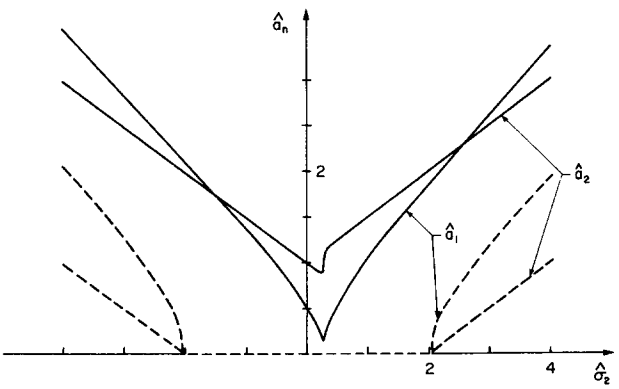

FIG. 2. Frequency-response curves for the case of principal parametric resonance of the first mode for $\sigma_1/f=0.266$ and $\mu_n/f=0.02$: Solid curves — stable; ---, unstable with at least one eigenvalue being positive.

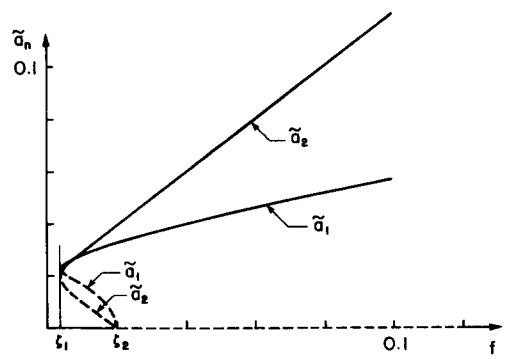

FIG. 4. Variation of the amplitudes $\tilde{a}_1$ and $\tilde{a}_2$ of the first and second modes with the amplitude f of the excitation for the case of principal parametric resonance of the first mode when there are two finite-amplitude solutions for $\mu_n=0.002$, $\sigma_1=0.0133$, and $\sigma_2=0.04$: Solid curves—stable; ---, unstable with at least one eigenvalue being positive.

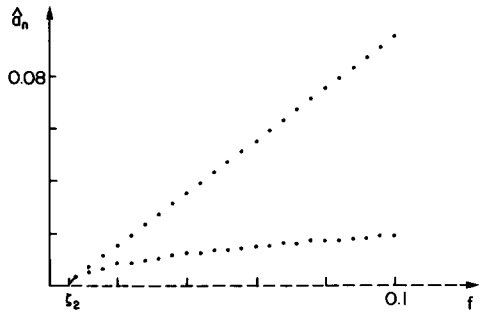

FIG. 5. Variation of the amplitudes $\tilde{a}_1$ and $\tilde{a}_2$ of the first and second modes with the amplitude f of the excitation for the case of principal parametric resonance of the first mode when there is only one finite-amplitude solution for $\mu_n = 0.002$, $\sigma_1 = 0.0133$, and $\sigma_2 = 0.01$: Solid curves — stable; ---, unstable with at least one eigenvalue being positive; $\cdots$, unstable with the real part of a c.c. pair of eigenvalues being positive.

the two saddles (corresponding to $\hat{a}_n$ and $-\hat{a}_n$) shrink toward the sink. As f increases beyond ζ_2, the sink becomes a saddle point.

Figure 5 shows the variation of the $\tilde{a}_n$ with f for a case in which a Hopf bifurcation exists. All the parameters in this case are the same as those in Fig. 4 except that $\sigma_2 = 0.01$. When $f \leqslant \zeta_2$, where $\zeta_2 \approx 0.0054$, there is only one trivial fixed point, namely, the trivial point, which is stable (sink). Consequently, the response is trivial. When $\zeta_2 < f < \zeta_3$, where $\zeta_3 \approx 0.0076$, there are two possible fixed points: a trivial point, which is unstable (saddle) and a nontrivial point, which is stable (sink). Consequently, the response is periodic and given by Eqs. (84) and (85). The point $f = \zeta_2$ is a supercritical pitchfork bifurcation point. As f increases past ζ_2, the sink becomes a saddle point and gives rise to two sinks (corresponding to $\hat{a}_n$ and $-\hat{a}_n$). When $f > \zeta_3$, there are two possible fixed points: a trivial point, which is unstable (saddle) and a nontrivial point, which is also unstable (unstable focus). Thus as f increases through ζ_3, the nontrivial fixed point loses its stability with a pair of complex eigenvalues

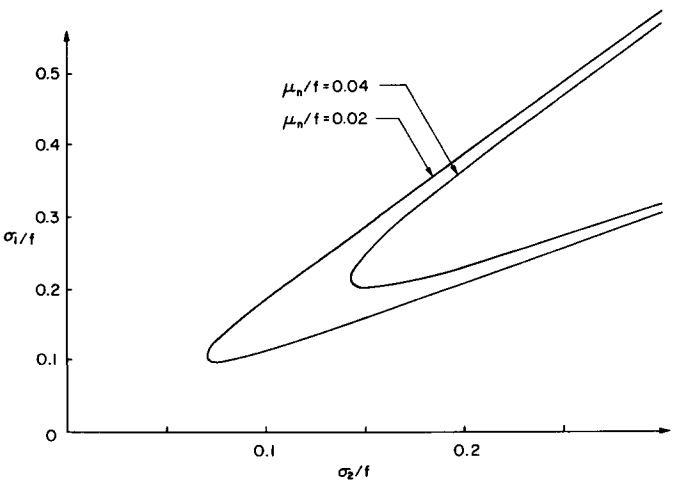

FIG. 6. Transition curves across which the real part of a c.c. pair of eigenvalues changes sign (it is positive inside the curves) for $\mu_n/f = 0.02$ and 0.04. We show the case of principal parametric resonance of the first mode.

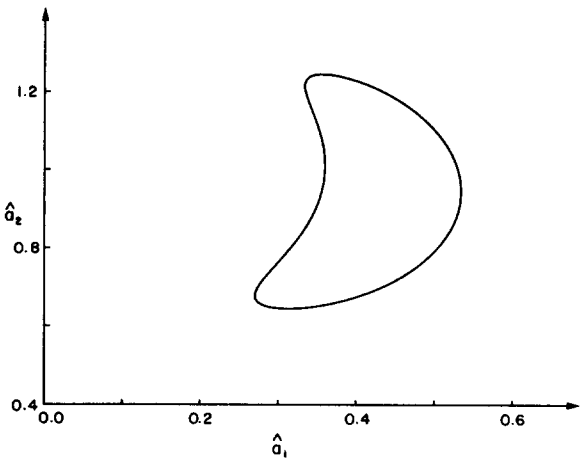

FIG. 7. Projection of the trajectory of the modulation equations for the case of principal parametric resonance of the first mode on the $\hat{a}_2$-$\hat{a}_1$ plane, where $\hat{a}_1 = a_1\sqrt{\Lambda_1}\Lambda_2/f$ and $\hat{a}_2 = a_2\Lambda_1/f$ for $\mu_n/f = 0.02$, $\sigma_1/f = 0.266$, and $\sigma_2/f = 0.15$. It exhibits a limit-cycle oscillation.

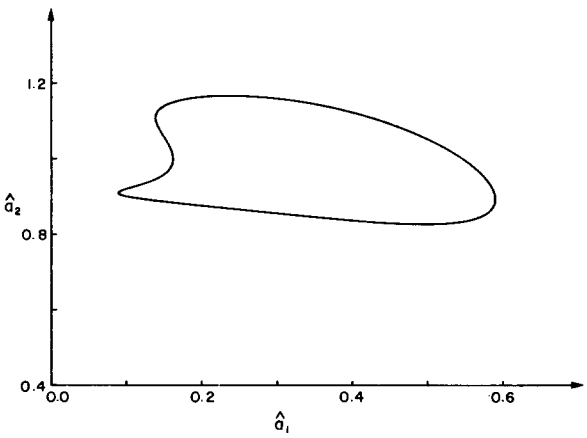

FIG. 8. Projection of the trajectory of the modulation equations for the case of principal parametric resonance of the first mode on the $\hat{a}_2$-$\hat{a}_1$ plane, where $\hat{a}_1 = a_1\sqrt{\Lambda_1}\Lambda_2/f$ and $\hat{a}_2 = a_2\Lambda_1/f$ for $\mu_n/f = 0.02$, $\sigma_1/f = 0.266$, and $\sigma_2/f = 0.20$. It exhibits a limit-cycle oscillation.

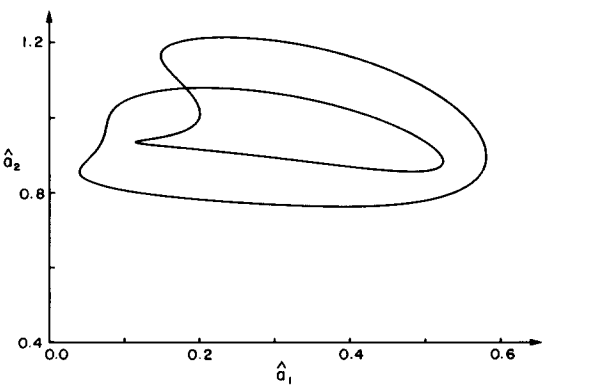

FIG. 9. Projection of the trajectory of the modulation equations for the case of principal parametric resonance of the first mode on the $\hat{a}_2$-$\hat{a}_1$ plane, where $\hat{a}_1 = a_1\sqrt{\Lambda_1}\Lambda_2/f$ and $\hat{a}_2 = a_2\Lambda_1/f$ for $\mu_n/f = 0.02$, $\sigma_1/f = 0.266$, and $\sigma_2/f = 0.21$. It exhibits a period 2 trajectory.

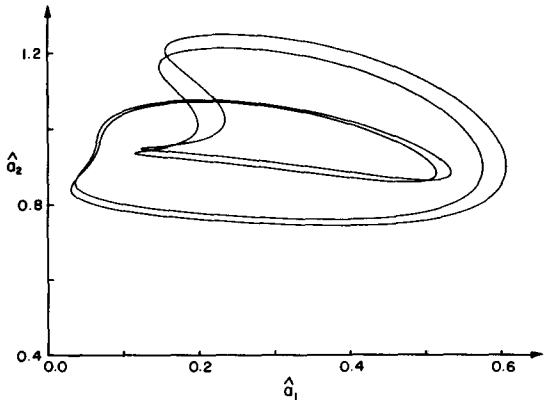

FIG. 10. Projection of the trajectory of the modulation equations for the case of principal parametric resonance of the first mode on the $\hat{a}_2$-$\hat{a}_1$ plane, where $\hat{a}_1 = a_1\sqrt{\Lambda_1}\Lambda_2/f$ and $\hat{a}_2 = a_2\Lambda_1/f$ for $\mu_n/f = 0.02$, $\sigma_1/f = 0.266$, and $\sigma_2/f = 0.2111$. It exhibits a period 4 trajectory.

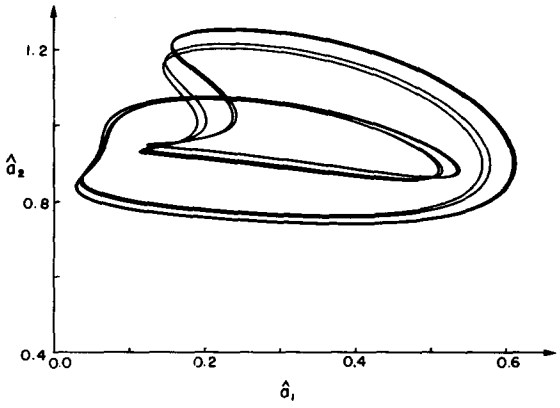

FIG. 11. Projection of the trajectory of the modulation equations for the case of principal parametric resonance of the first mode on the $\hat{a}_2$-$\hat{a}_1$ plane, where $\hat{a}_1 = a_1\sqrt{\Lambda_1}\Lambda_2/f$ and $\hat{a}_2 = a_2\Lambda_1/f$ for $\mu_n/f = 0.02$, $\sigma_1/f = 0.266$, and $\sigma_2/f = 0.21125$. It exhibits a period 8 trajectory.

crossing the imaginary axis into the right half of the complex plane, and hence $f = \zeta_3$ is a Hopf bifurcation point. Based on the Hopf bifurcation theorem,[22] near ζ_2 the evolution equations have limit cycle solutions with amplitudes proportional to $|f - \zeta_3|^{1/2}$, corresponding to a 2-D torus of the original system.

As mentioned earlier, Miles[5] examined the case of perfect internal resonance (i.e., $\omega_2 = 2\omega_1$ or $\sigma_1 = 0$) for this case and for the case of a double pendulum[21] and did not find Hopf bifurcations, in agreement with the present results. However, the present analysis shows that if the condition of perfect internal resonance is relaxed, then Hopf bifurcations are possible. When $\hat{\mu}_n = \mu_n/f = 0.02$ and 0.04, Fig. 6 shows the transition curves in the plane $\hat{\sigma}_2$-$\hat{\sigma}_1$, where $\hat{\sigma}_n = \sigma_n/f$, across which the real part of a c.c. pair of eigenvalues changes sign; hence these curves correspond to Hopf bifurcations. The real part is positive inside the curves. Based on the Hopf bifurcation theorem,[22] we expect the modulation equations to exhibit limit-cycle oscillations near these transition curves. An example is shown in Fig. 7. Figure 7 shows the projection of the trajectory of the modulation equations on the $\hat{a}_2$-$\hat{a}_1$ plane, where $\hat{a}_1 = a_1\sqrt{\Lambda_1\Lambda_2}/f$ and $\hat{a}_2 = a_2\Lambda_1/f$ for $\hat{\mu}_n = 0.02$, $\hat{\sigma}_1 = 0.266$, and $\hat{\sigma}_2 = 0.15$. Similar results were obtained by Nayfeh[23] for the case of a double pendulum.

Keeping all parameters in Fig. 7 fixed at $\hat{\mu}_n = 0.02$ and $\hat{\sigma}_1 = 0.266$ and increasing the control parameter $\hat{\sigma}_2$, we find that the limit cycle increases at first, then decreases, and finally loses its stability through a period-doubling flip bifurcation (see Figs. 8–11), culminating in what appears to be a chaotic motion. Then, the solutions of the averaged equations undergo a reverse bifurcation back to a fixed point for sufficiently large values of $\hat{\sigma}_2$.

ACKNOWLEDGMENT

This work was supported by the National Science Foundation under Grant No. MSM-8521748.

[1]M. Faraday, Philos. Trans. R. Soc. London **121**, 299 (1831).
[2]Lord Rayleigh, Philos. Mag. **16**, 50 (1833).
[3]T. B. Benjamin and F. Ursell, Proc. R. Soc. London, Ser. A **225**, 505 (1954).
[4]F. T. Dodge, D. D. Kana, and H. N. Abramson, AIAA J. **3**, 685 (1965).
[5]J. W. Miles, J. Fluid Mech. **146**, 285 (1984).
[6]W. Henstock and R. L. Sani, Lett. Heat Mass Trans. **1**, 95 (1974).
[7]J. R. Ockendon and H. Ockendon, J. Fluid Mech. **59**, 397 (1973).
[8]V. K. Melnikov, Trans. Moscow Math. Soc. **12**, 1 (1963).
[9]P. Holmes, J. Fluid Mech. **162**, 365 (1986).
[10]J. W. Miles, J. Fluid Mech. **75**, 419 (1976).
[11]R. Keolian, L. A. Turkevich, S. J. Putterman, and I. Rudnick, Phys. Rev. Lett. **47**, 1133 (1981).
[12]J. P. Gollub and C. W. Meyer, Physcia D **6**, 337 (1983).
[13]R. Keolian and I. Rudnick, in *Frontiers in Physical Acoustics*, edited by D. Sette (1984).
[14]S. Ciliberto and J. P. Gollub, Phys. Rev. Lett. **52**, 922 (1984).
[15]S. Ciliberto and J. P. Gollub, J. Fluid Mech. **158**, 381 (1985).
[16]A. H. Nayfeh, *Perturbation Methods* (Wiley-Interscience, New York, 1973).
[17]A. H. Nayfeh, *Introduction to Perturbation Techniques* (Wiley-Interscience, New York, 1981).
[18]A. H. Nayfeh and D. T. Mook, *Nonlinear Oscillations* (Wiley-Interscience, New York, 1979).
[19]L. R. Mack, J. Geophys. Res. **67**, 829 (1962).
[20]J. W. Miles, J. Fluid. Mech. **149**, 1 (1984).
[21]J. W. Miles, Z. Angew. Math. Phys. **36**, 338 (1985).
[22]J. K. Hale, *Oscillations in Nonlinear Systems* (McGraw-Hill, New York, 1963).
[23]A. H. Nayfeh, J. Sound Vib., in press.